

AEDC-TR-66-135

ARCHIVE COPY  
DO NOT LOAN

ayl



**DESCRIPTION AND PERFORMANCE OF A  
MOLECULAR BEAM CHAMBER USED FOR  
CRYOPUMPING AND ADSORPTION PUMPING STUDIES**

R. F. Brown and J. H. Heald, Jr.  
ARO, Inc.

**October 1966**

Distribution of this document is unlimited.

**AEROSPACE ENVIRONMENTAL FACILITY  
ARNOLD ENGINEERING DEVELOPMENT CENTER  
AIR FORCE SYSTEMS COMMAND  
ARNOLD AIR FORCE STATION, TENNESSEE**

AEDC TECHNICAL LIBRARY



TESE TE000 0240 5

PROPERTY OF U. S. AIR FORCE  
AEDC LIBRARY  
AF 40(600)1200

# ***NOTICES***

When U. S. Government drawings, specifications, or other data are used for any purpose other than a definitely related Government procurement operation, the Government thereby incurs no responsibility nor any obligation whatsoever, and the fact that the Government may have formulated, furnished, or in any way supplied the said drawings, specifications, or other data, is not to be regarded by implication or otherwise, or in any manner licensing the holder or any other person or corporation, or conveying any rights or permission to manufacture, use, or sell any patented invention that may in any way be related thereto.

Qualified users may obtain copies of this report from the Defense Documentation Center.

References to named commercial products in this report are not to be considered in any sense as an endorsement of the product by the United States Air Force or the Government.

DESCRIPTION AND PERFORMANCE OF A  
MOLECULAR BEAM CHAMBER USED FOR  
CRYOPUMPING AND ADSORPTION PUMPING STUDIES

R. F. Brown and J. H. Heald, Jr.  
ARO, Inc.

Distribution of this document is unlimited.

## FOREWORD

The research presented in this report was sponsored by the Arnold Engineering Development Center (AEDC), Air Force Systems Command (AFSC), Arnold Air Force Station, Tennessee, under Program Element 61445014, Project 8951.

The results presented were obtained by ARO, Inc. (a subsidiary of Sverdrup & Parcel and Associates, Inc.), contract operator of the AEDC under Contract AF 40(600)-1200. The research was conducted from June 1965 to May 1966 under ARO Projects SW3417 and SW2606. The manuscript was submitted for publication on June 21, 1966.

This technical report has been reviewed and is approved.

James G. Mitchell  
Chief, Advanced Plans Division  
Directorate of Plans and Technology

Donald R. Eastman  
Acting Director  
Directorate of Plans and Technology

### ABSTRACT

An aerodynamic molecular beam chamber has been constructed and operated at Arnold Engineering Development Center. Design criteria, performance data, and space simulation applications are discussed in this report. Cryopumping was used to provide the required pumping speed and to reduce the scattering of the beam by the background gas. A maximum beam intensity of  $2.0 \times 10^{20}$  CO<sub>2</sub> molecules per second per steradian was measured. It was determined that a two-fold increase in the beam intensity can be obtained by cryogenically cooling the skimmer, and the range of source pressures over which this occurs was established for one configuration of the beam components. A modulated beam detector capable of extracting weak reflected beam signals from the background noise has been developed. The beam and detector are now being used to study basic cryopumping phenomena on a microscopic scale and to provide capture coefficient data for immediate application in the design of cryopumping systems for space simulation chambers.

## CONTENTS

	<u>Page</u>
ABSTRACT . . . . .	iii
NOMENCLATURE . . . . .	vi
I. INTRODUCTION . . . . .	1
II. BACKGROUND AND THEORY OF OPERATION . . . . .	1
III. DESIGN CRITERIA . . . . .	4
IV. APPARATUS . . . . .	5
V. PROCEDURE . . . . .	8
VI. DISCUSSION . . . . .	8
VII. CONCLUDING REMARKS . . . . .	15
REFERENCES . . . . .	15

## ILLUSTRATIONS

### Figure

1. Oven Beam Generator . . . . .	17
2. Aerodynamic Beam Generator . . . . .	17
3. Molecular Beam Chamber . . . . .	18
4. Schematic of Aerodynamic Molecular Beam Chamber . . . . .	19
5. Molecular Beam Detector . . . . .	20
6. Typical CO <sub>2</sub> Beam Performance Data . . . . .	21
7. Effect of Nozzle-Skimmer Separation Distance, CO <sub>2</sub> . . . . .	22
8. Background Gas Scattering for 100-torr CO <sub>2</sub> Source Pressure . . . . .	23
9. Cold Skimmer Effects, CO <sub>2</sub> . . . . .	24
10. Beam Performance with Variable Skimmer Temperature, CO <sub>2</sub> . . . . .	25

## TABLE

1. Typical Test Data . . . . .	26
--------------------------------	----

## NOMENCLATURE

$A_s$	Source orifice area in an oven beam or skimmer entrance area in an aerodynamic beam, $\text{cm}^2$
$C$	Capture coefficient, nondimensional
$d_c$	Collimator orifice diameter, mm
$d_n$	Sonic nozzle exit diameter, mm
$d_s$	Skimmer entrance diameter, mm
$I$	Aerodynamic beam intensity, $\text{molecules/sec/cm}^2$
$I_o$	Oven beam intensity, $\text{molecules/sec/cm}^2$
$I_{rc}$	Reflected beam intensity entering detector gage from surface cooled to desired testing temperature, $\text{molecules/sec/cm}^2$
$I_{rw}$	Reflected beam intensity entering detector gage from surface sufficiently warm to prevent beam condensation, $\text{molecules/sec/cm}^2$
$K_d$	Detector gage calibration constant, $\text{molecules/sec/unit}$ detector reading
$K_n$	Knudsen number, nondimensional
$k$	Boltzmann constant, $\text{ergs/}^\circ\text{K}$
$\ell_{sc}$	Source to collimator distance in oven beam or skimmer to collimator distance in aerodynamic beam, cm
$M_s$	Mach number of the gas flow at the skimmer entrance, nondimensional
$\dot{N}$	Beam flux, $\text{molecules/sec}$
$\dot{N}_i$	Total beam flux incident on a test surface, $\text{molecules/sec}$
$\dot{N}_r$	Total beam flux reflected from a test surface, $\text{molecules/sec}$
$n_o$	Gas density in source plenum, $\text{molecules/cm}^3$
$n_s$	Molecular density at skimmer entrance, $\text{molecules/cm}^3$
$P_c$	Gas pressure in collimating chamber, torr
$P_n$	Gas pressure in nozzle discharge chamber, torr
$P_o$	Gas pressure in source plenum, torr
$P_t$	Gas pressure in test chamber, torr
$\Delta P_d$	Ionization gage response reading to a given beam flux, torr

$T_o$	Gas temperature in source gas plenum, °K
$v_{\max}$	Maximum hydrodynamic velocity in a free jet expansion, cm/sec
$\bar{v}_o$	Mean molecular velocity in the oven of an oven beam, cm/sec
$\gamma$	Ratio of specific heats, nondimensional
$\delta$	Nozzle-skimmer separation distance, nozzle diameters
$\lambda_s$	Mean free path at skimmer entrance, mm



## SECTION I INTRODUCTION

The purpose of this report is to discuss the design and performance of a molecular beam chamber and also its application to studies of basic cryopumping and adsorption pumping mechanisms.

At the Arnold Engineering Development Center (AEDC) and at other laboratories, investigations of the cryopumping mechanism have been in progress for several years, and useful engineering data have been collected. However, these studies have been limited to investigations of the pumping speeds of the various gases on engineering surfaces.\* The available data do not furnish sufficient fundamental information about the basic condensation process to allow formulation of empirical or theoretical methods for predicting the capture coefficient of a cryosurface for all test gases. In addition, previous investigations have been limited to a narrow range of the possible experimental variables. The need for a wide range of experimental cryopumping data occurs frequently in space simulation and testing. For instance, in order to determine if the exhaust products from a small rocket firing can be removed from a space simulation chamber by cryopumping, knowledge of the capture coefficient of directed flow high temperature gas is required. Adequate data of this type are not available.

Molecular beam techniques can not only be used to provide engineering data of this type, but also they can be used to investigate the basic condensation process on the microscopic scale. Consequently, a high intensity molecular beam chamber of the Kantrowitz and Grey type (Ref. 1) has been constructed and is now in operation at AEDC. The apparatus is being used to study basic gas surface interaction processes and to provide experimental capture coefficient data.

## SECTION II BACKGROUND AND THEORY OF OPERATION

The first use of the molecular beam technique is attributed to Dunoyer, who in 1911 demonstrated the rectilinear motion of sodium atoms in a vacuum. Since that time molecular beam experiments have

---

\*Any surface which is not microscopically defined or is not free from background gas contamination.

been widely used in fundamental studies of atoms, molecules, and nuclei (Ref. 2). Molecular beam techniques are now being widely used to study the energy and momentum exchange between a neutral gas and a solid surface. The use of a molecular beam to study the condensation of a neutral gas on a solid surface is simply an extension of these techniques.

Several methods have been used for the generation of molecular beams, but the classical oven beam system has been the most widely used method to date. Since 1951, however, the method of aerodynamic molecular beam generation, as suggested by Kantrowitz and Grey (Ref. 1), has been widely used.

Figure 1 is a schematic representation of a classical oven beam system. The beam gas originates in the oven, so-called because many experimental gases have been produced by the vapor of heated substances. Gas from the oven passes into the high vacuum region of a collimating chamber through a thin walled orifice or slit. The gas flow from this orifice will be effusive (i. e., random molecular motion with no inter-molecular collisions in the vicinity of the orifice) if the mean free path of the gas in the oven is greater than the diameter of the orifice. Under these conditions, the flux vectors of the molecules which effuse from the orifice will be contained in a spherical shell represented by the dashed circle in Fig. 1. A collimator orifice placed coaxially with the source orifice will then allow only those gas molecules to pass which have trajectories within the solid angle formed by these two orifices. The molecular beam consists of this collimated gas flow entering the test chamber. From the kinetic theory relations for equilibrium molecular flux, the intensity of the molecular flow entering the test chamber is given by

$$I_o = \frac{n_o \bar{v}_o A_s}{4\pi l_{sc}^2} \quad (1)$$

The advantages of oven beam generation are that a beam of known intensity and energy can be produced and that a vacuum system of simple construction with modest pumping speeds can be used. The main disadvantage is the relatively low beam intensity which severely limits the measurement of reflected beams in gas-surface interaction studies.

To help overcome this limitation Kantrowitz and Grey (Ref. 1) in 1951 suggested replacing the effusive flow source of the classical oven beam with a supersonic jet. The basic elements of such a molecular beam generator are shown in Fig. 2. For comparison, the skimmer can be considered as the first defining orifice for the beam just as the source orifice functioned in the oven beam. The difference between the two

systems arises from the fact that in the aerodynamic beam the gas is accelerated during the gas expansion process between the nozzle and skimmer while in the oven beam the gas in the oven approaches the source orifice only by random molecular motion. This acceleration process serves to increase the aerodynamic beam intensity in two ways:

1. The mass flow per unit area through the skimmer will be greater for a given molecular density.
2. The fraction of the total mass flow passing through the skimmer that passes through the collimator is greater than in the oven beam system.

Parker et al. (Ref. 3) have refined the original derivation of Kantrowitz and Grey for the theoretical beam intensity in an aerodynamic beam based on the following assumptions:

1. The flow between the nozzle exit and skimmer entrance is isentropic and obeys the ordinary continuum flow theory.
2. The flow into the skimmer entrance is supersonic and undisturbed by the presence of the skimmer.
3. The flow downstream of the skimmer is free molecular--i. e., no molecular collisions occur.

The results of the Kantrowitz-Grey derivation as refined by Parker et al. can be written in a form to permit direct comparison with the theoretical intensity of an oven beam:

$$I = \frac{n_s v_{max} A_s (3 + \gamma M_s^2)}{2\pi r_{sc}^2} \quad (2)$$

Comparison of Eq. (2) with Eq. (1) indicates that the ratio of aerodynamic beam intensity to oven beam intensity is

$$\frac{I}{I_o} = \frac{2v_{max}}{v_o} (3 + \gamma M_s^2) \text{ for } n_s = n_o \quad (3)$$

For a ratio of specific heats of 1.4 and a Mach number of 4, this ratio is 75; and for a Mach number of 10, this ratio is 465. In practice, the aerodynamic beam intensities are generally one to two orders of magnitude greater than oven beam intensities with equal molecular densities at the oven beam orifice and aerodynamic beam skimmer.

The advantages of aerodynamic molecular beam generation are greater beam intensities and narrower velocity distributions. The main

difficulty in producing a high intensity aerodynamic molecular beam is the requirement for a vacuum system with very high pumping speed and its associated higher costs.

### SECTION III DESIGN CRITERIA

In using molecular beam techniques to study gas-surface interactions, the main difficulty is obtaining a beam with sufficient flux to allow measurement of the reflected beam parameters--i. e., energy and flux. This makes it desirable to increase both the beam intensity--i. e., flux per unit area--and the total beam flux for particle-surface interaction studies.

The AEDC molecular beam was designed to attain the following characteristics:

1. A molecular beam with a high intensity and a narrow velocity distribution (This was attained by the utilization of the aerodynamic beam characteristics.)
2. An additional increase in the beam intensity (Cryopumping was used to decrease the beam dissipation by background gas scattering.)
3. An increase in the total beam flux (Cryopumping makes possible the use of larger skimmers and collimators and higher source pressures.)
4. A highly collimated beam (This is attained by operating at higher collimation distances and was made possible by the use of cryopumping to reduce the gas background.)
5. A low background gas pressure in the test chamber (This makes it possible to detect weak reflected beam signals and was accomplished by the use of cryopumping.)
6. The capability of producing beams with energies from 0.01 to 3 ev (This is to be achieved during the second phase of the AEDC beam program by resistance heating of the source to produce energies from 0.1 to 0.5 ev and by using an arc jet to produce energies of 3 ev (Ref. 4).)

During the design of the AEDC molecular beam system several problems were anticipated as the result of the extensive use of cryogenic pumping. However, only two minor problems were encountered when the cell was operated. First, the gas temperature in the nozzle supply plenum

decreased approximately 10°K per hour. Second, the micro-manipulator movement mechanism froze after three hours of operation. Both problems were eliminated by insulating with two layers of aluminum foil and using a 20-w resistance heater. Another problem that had been anticipated during the design was that the beam components (i. e., nozzle, skimmer, and collimator) would have to be realigned after the cryoliners were cooled from 300°K to cryogenic temperatures. During the performance test, the alignment was checked several times as the cryoliners were cooled from 300 to 77°K and no change in the alignment was detected.

## SECTION IV APPARATUS

### 4.1 CHAMBER CONSTRUCTION

The molecular beam cell, as shown in Figs. 3 and 4, is a stainless steel cylinder 3 ft in diameter by 6-1/2 ft long which is subdivided into three sections by two removable bulkheads. The first bulkhead separates the nozzle section of the cell from the collimation section and serves as a mounting base for the beam skimmer. The beam collimating orifice is mounted on the second bulkhead which separates the collimation and test sections of the cell. Standard high vacuum construction was used throughout the chamber, and a vacuum of  $10^{-9}$  torr has been produced and maintained.

The nozzle-skimmer separation distance can be changed without breaking the vacuum. This was accomplished by mounting the nozzle and gas supply plenum on a micro-manipulator with x, y, and z movements. The micro-manipulator is moved by a flexible shaft drive mechanism that is attached to a rotary feedthrough at the cell wall.

### 4.2 PUMPING SYSTEMS

Vacuum conditions are produced and maintained in the cell by (1) three separate oil diffusion pumping systems (i. e., one for each section of the cell), (2) gaseous-helium (GHe)-cooled, 20°K cryoliners, and (3) liquid-nitrogen (LN<sub>2</sub>)-cooled, 77°K cryoliners. Typical pumping speeds and operating pressures for the system are shown in the following table.

Chamber Section	Pumping System	Nominal Pumping Speed, liters/sec	Operating Pressure, torr
Nozzle-Discharge	(1) 16-in. oil diffusion pump (2) Gaseous-He-cooled cryoliner, 20°K (3) Liquid-nitrogen-cooled cryoliner, 77°K	2,000* 270,000* 270,000**	$10^{-4}$ to $10^{-7}$
Collimation	(1) 10-in. oil diffusion pump (2) Gaseous-He-cooled cryoliner, 20°K (3) Liquid-nitrogen-cooled cryoliner, 77°K	2,000* 185,000* 200,000**	$10^{-6}$ to $10^{-7}$
Test	(1) 10-in. oil diffusion pump (2) Gaseous-He-cooled cryopanel, 20°K (3) Liquid nitrogen cryosphere, 77°K	2,000* 40,000* 8,000**	$10^{-8}$ to $10^{-9}$

\* Pumping speed for air

\*\* Pumping speed for CO<sub>2</sub>

The 77 and 20°K cryoliners used in the nozzle and collimation sections of the cell are cylinders fabricated by welding copper tubing to 1/8-in. copper sheet. The 20°K cylinder nestles inside the 77°K cylinder and is isolated from it by Teflon® spacers. One of the cylinder ends is omitted on both the 77 and the 20°K cryoliners for the nozzle section to provide access through the end of the cell to the nozzle and skimmer when the cryoliners are installed. During operation at 20°K, two layers of foiled-backed Mylar® are used to reduce heat transfer from the 300°K end flange to the 20°K cryoliner.

All connections of supply and exhaust lines to the 77 and 20°K cryoliners are made with external bayonet fittings. This allows the use of LN<sub>2</sub> for cooling both the inner and outer cryoliners to 77°K for test gases such as CO<sub>2</sub>, and the change from one cryogenic coolant to another can be made without breaking the cell vacuum.

#### 4.3 BEAM GENERATING COMPONENTS

The beam components used during the performance test are given on the following page.

Beam Components	Description	Material	Diameter, mm
Nozzle	Conical sonic orifice	Brass	0.5
Skimmer	Hollow cone with truncated tip. simivertex angles of 30 deg internal and 40 deg external	Aluminum	2
Collimator	Thin wall orifice	Aluminum	4

#### 4.4 GAS ADDITION SYSTEM

The beam gas is supplied to the 50-cc gas plenum inside the cell by a 0.5-in. -diam flexible line that penetrates the cell wall and attaches to a 1-liter surge tank on the outside of the cell. Gas is delivered to the surge tank from standard gas bottles through a needle valve. The plenum pressure,  $P_0$ , is measured by an Alphatron® and a Bourdon-tube-type, pressure gage attached to the 1-liter surge tank.

#### 4.5 CHAMBER PRESSURE MEASURING DEVICES

Bayard-Alpert ionization gages for monitoring the cell pressure are mounted on ports located on the top and near the center of each section of the cell. A 2-in. -diam stainless steel tube extends from the gage opening down through an opening in the cryoliner. This arrangement permits the use of the gage to measure the molecular density in the cell with no interference from the adjacent cryoliner. However, extreme pressure gradients undoubtedly exist in the nozzle section of the cell when the beam is operating with cold cryoliner.

The beam detector used during the performance test was a miniature (25-mm-diam) Bayard-Alpert ionization gage mounted in the configuration shown in Fig. 5. A thin wall, 6-mm-diam orifice was used to reduce the influence of the chamber background gas.

The beam detector gage was calibrated by using an oven molecular beam as the source of a known beam flux,  $N$ . The gage constant,  $K_d$ , was determined from

$$K_d = \frac{\dot{N}}{\Delta P_d} \quad (4)$$

The beam deflector, as shown in Fig. 5, is a metal disk four inches in diameter. The beam is turned off with respect to the detector gage by moving the beam deflector to a position where it intercepts the beam.

## SECTION V PROCEDURE

The alignment of the beam-components (i. e. , nozzle, skimmer, and collimator) is accomplished by using a transit to establish an axis and then mounting each of the components on this axis.

After alignment is completed, the cell is evacuated to a pressure of  $10^{-8}$  torr, and the procedure for producing the beam is as follows:

1. The nozzle is moved along the horizontal axis until the desired nozzle-skimmer separation distance is obtained.
2. The beam test gas is admitted to the nozzle supply plenum and the desired pressure is established.
3. Readings of the detector gage are made with the beam off and on to obtain the value of  $\Delta P_d$  in torr.
4. The beam flux in molecules per second is obtained using Eq. (4).

## SECTION VI DISCUSSION

### 6.1 PERFORMANCE TEST RESULTS

A series of beam performance test runs was made with the nozzle-skimmer separation distance varied from 5 to 117 nozzle diameters and with source pressures varied from 1 to 3400 torr. During these tests,  $\text{CO}_2$  was used as the beam gas, and the cryoliner was maintained at 77°K. The maximum beam intensity measured during the performance test was  $2.0 \times 10^{20}$   $\text{CO}_2$  molecules per second per steradian\* at a source pressure of 3400 torr and a nozzle-skimmer separation distance of

---

\*Beam intensities are reported in steradian units determined by the solid angle of the collimator with respect to a point source at the skimmer entrance.



20 nozzle diameters. Low background pressures were maintained in each of the three sections of the cell during all of the runs, and data from a typical run at a nozzle-skimmer separation distance of 60 nozzle diameters are presented in Fig. 6 and Table I. The low chamber operating pressures indicate that the AEDC molecular beam could be operated at a source pressure of 45 atm (34,000 torr) and that the pumping system would maintain a vacuum lower than those reported by previous investigators. Fenn et al. (Ref. 5) reported operating pressures of  $10^{-3}$  to  $10^{-4}$  torr in the nozzle section and pressures of  $10^{-5}$  to  $10^{-6}$  torr in the collimation section of the Princeton molecular beam cell. Source pressures at AEDC thus far have been limited to 5300 torr by the gas addition system.

As shown in Fig. 6, the beam flux increases to a relative maximum, decreases to a relative minimum, and then continues to increase as the source pressure is continually increased. These changes in the total beam flux are related to the flow conditions at the skimmer entrance. At the low source pressures, 10 to 108 torr, free-molecule flow conditions predominate, and the total beam flux increases with source pressure. Then as the pressure is increased, the flow field at the skimmer entrance changes from free molecular to continuum. This transition is characterized by a decrease followed by a rapid increase in the beam flux at the higher source pressures.

Although several investigators are studying the interaction of the skimmer with a rarefied gas flow, the effects of the skimmer on the beam intensity have not been adequately explained. The available data indicate that changing viscous effects at the skimmer during transition are responsible for the observed decrease in the beam intensity.

Another possible occurrence that should be considered when operating at the higher source pressures is condensation in the beam. Bier and Hagen (Ref. 6) have reported condensed clusters of molecules in aerodynamic molecular beams produced by expanding  $\text{CO}_2$  from source pressures greater than 300 torr. This has been supported by the more recent work of Green and Milne (Ref. 7). It has not been determined if condensation occurs in the AEDC beam. However, the rapid increase in the measured beam flux at source pressures greater than 300 torr could be partially attributed to condensation in the beam. Future work at AEDC will include the use of a mass spectrometer to determine the onset of condensation.

Another set of the AEDC beam performance data is shown in Fig. 7. Again, the advantages of using cryopumping are evident, as the beam

intensity remains high at large nozzle skimmer separation distances. Previous investigators (Refs. 5 and 8) have reported similar data, having the same general characteristics as that shown in Fig. 7 but with a rapid decrease in the intensity at nozzle skimmer separation distances greater than 50 nozzle diameters. This observed decrease in beam intensity at high nozzle-skimmer separation distance has been attributed to the excessive pressures in the nozzle and collimation sections of the chambers. The AEDC data support this conclusion. (The theoretical curves shown in Figs. 6 and 7 have been computed from the theory of Ref. 3 using the Mach numbers from the calculations of Sherman, Ref. 9.)

This theory is plotted in Fig. 6 for specific heat ratios of 1.30, 1.40, and 1.67. At room temperature and standard conditions, CO<sub>2</sub> has a specific heat ratio of 1.28 (Ref. 10). However, in a free-jet expansion of CO<sub>2</sub>, the internal degrees of freedom are not expected to share equally in the partition of energy, and a specific heat ratio that changes from 1.28 at high source pressures to 1.67 at low source pressures would better describe the conditions (Ref. 11).

#### 6.1.1 Background Gas Scattering

As discussed in Section III, cryopumping was utilized in the AEDC molecular beam chamber to minimize the loss in beam intensity caused by background gas scattering. In the collimation and test chambers, operating pressures (Table I) are sufficiently low to insure negligible scattering of the beam between the skimmer and detector (Ref. 3). However, as shown by Anderson and Fenn (Ref. 12), under certain operating conditions the background gas in the nozzle discharge chamber can penetrate to the axis of the free jet expansion from the nozzle. This results in the scattering of beam producing gas in the region between the nozzle and skimmer.

Several experiments have been conducted to determine the magnitude of this scattering, the operating conditions under which it occurs, and the reduction in scattering provided by the system's high cryopumping speeds. At constant source pressure and background gas pressure, the nozzle-skimmer separation distance was varied and the change in beam intensity observed. In this manner experiments were conducted at background pressures from  $6 \times 10^{-3}$  torr to  $3 \times 10^{-5}$  torr, and at source pressures from 5 to 600 torr.

Figure 8 shows the results obtained for a 100-torr source pressure CO<sub>2</sub> beam. At nozzle-skimmer separation distances greater than the relative maximum points (35-40 nozzle diameters), the beam intensity is strongly dependent on the background gas pressure. At the high separation

distances in Fig. 8, an order of magnitude reduction in background gas pressure (from  $6 \times 10^{-3}$  to  $6 \times 10^{-4}$  torr) can result in an order of magnitude increase in beam intensity.

The data taken at a background gas pressure of  $6.3 \times 10^{-4}$  torr represent normal operating conditions with the cryogenic liners cooled. The data for the other three curves of Fig. 8 were taken with the cryogenic liners warm and  $\text{CO}_2$  gas bled into the nozzle discharge chamber to vary the background pressure. The advantage of cryopumping is readily apparent. Substantial increases in beam intensity have been observed for reductions in nozzle discharge chamber pressure below  $10^{-4}$  torr.

### 6.1.2 Skimmer Interactions

Experiments have been conducted to determine the magnitude of skimmer interaction effects on beam intensity and also the range of these effects in terms of the density level at the skimmer entrance. As reported by Mayer et al. in Ref. 13, viscous effects such as shock waves and boundary layers in aerodynamic flows can be virtually eliminated by cryogenically cooling the surface which interacts with the flow field.

A skimmer, cryogenically cooled to liquid nitrogen temperature ( $77^\circ\text{K}$ ), was used to intercept a room temperature  $\text{CO}_2$  gas flow which readily condenses when striking a surface at that temperature. In the first experiment, the skimmer was slowly cooled from room temperature to  $77^\circ\text{K}$ , and the beam flux was observed as a function of time. The source pressure and nozzle-skimmer separation distance were chosen to place the skimmer in the transition region between free molecular flow and fully established continuum flow. The results of this experiment are shown in Fig. 9. Very little change in beam flux occurs until the skimmer entrance is sufficiently cold to condense the  $\text{CO}_2$  beam (visually observed), at which time a rapid increase in beam flux is observed. The beam flux increases by about 180 percent of the room temperature skimmer value, holds this value for only a few seconds, and then rapidly decreases. The decrease in beam flux is a result of  $\text{CO}_2$  condensate filling the skimmer entrance. This was determined by visually measuring the change in skimmer diameter during the experiment. That the entrance area of the skimmer decreases at approximately the same rate as beam flux is shown by the plot of skimmer entrance diameter squared in Fig. 9.

The increase in beam flux caused by cooling the skimmer was measured as a function of gas density at the skimmer entrance. At a constant nozzle-skimmer separation distance, the density at the skimmer

entrance was varied by changing the source pressure. The increase in beam flux was then observed at each source pressure as the skimmer was cooled from room temperature to 77°K. The results of this experiment are shown in Fig. 10. It is apparent that the increase in beam flux caused by cryogenically cooling the skimmer in this manner is confined to a finite range of gas density at the skimmer entrance. For the particular experiment shown in Fig. 10, the increase in beam flux occurs over a range of skimmer entrance Knudsen numbers from 16 to 0.32. (Knudsen number is computed from hard sphere cross sections and referenced to skimmer entrance diameter.) From the data of Figs. 9 and 10 it is apparent that the increase in beam intensity attributable to cooling the skimmer is restricted in time duration and density range at the skimmer entrance.

An interesting phenomenon is shown in Fig. 10. Very definite relative maximum and minimum points occur which are shifted to higher values of source pressure as the skimmer is cooled from room temperature to 77°K. In addition, the curves seem to merge at the higher source pressures. By observing the rate of change of beam flux as the skimmer entrance would fill with condensate (taken from measurements as shown in Fig. 9), it is suspected that the condensation efficiency of the skimmer entrance decreases at the higher source pressures. This may account for the tendency of the two curves in Fig. 10 to merge at the higher source pressures.

The possible occurrence of more than one gas dynamic phenomenon in the region of the relative maximum-minimum points of Fig. 10 preclude any definite conclusion on the cause of these characteristic shapes. Nonetheless, a twofold increase in beam intensity is possible by cryogenically cooling the skimmer, and the range of this increase has been established.

## 6.2 CAPTURE COEFFICIENT MEASUREMENTS

At AEDC, molecular beam techniques will be used to investigate gas cold surface interactions--i.e., cryopumping. A molecular beam is ideally suited for studies of the interaction between a solid surface and impinging gas molecules since a direct measurement of gas properties before and after collision with the surface is possible. In addition, separate control of beam gas, background gas, and surface properties is possible. For the cryopumping studies, the rate of condensation of a molecular beam impinging on a test surface will be measured as a function of (1) gas species, energy, and intensity; (2) test surface temperature, composition, and orientation relative to the beam;

and (3) background gas species and pressure. It is anticipated that beam energies will range from room temperature to the rocket exhaust level, and surface temperatures from room temperature to 4°K.

If the test surface is suspended to intercept the molecular beam and the reflected gas flux is compared to the incident beam flux, then the rate of condensation is given by the capture coefficient relation:

$$C = 1 - \frac{\dot{N}_r}{\dot{N}_i} \quad (5)$$

To simplify the measuring process and to avoid absolute measurement of the total incident and reflected beam flux, the capture coefficient can also be determined by measuring the relative change in reflected beam intensity entering the detector as the surface is cooled to the desired testing temperature, e. g. ,

$$C = 1 - \frac{I_{cr}}{I_{rw}} \quad (6)$$

This relation is applicable only if the spatial distribution of the reflected molecules remains constant with changing surface temperature and if negligible molecules are condensed while the surface is warm. The reflected beam patterns will be experimentally determined, and the reference intensity measurement,  $I_{rw}$ , will be obtained with the test surface sufficiently warm to insure negligible condensation.

## 6.2.1 Detector

### 6.2.1.1 Detector Requirements

In principle, a direct measurement and simple calculation of capture coefficient as defined by Eq. (6) is possible. However, the magnitude of the reflected beam intensity entering the detector will generally be less than the intensity of background gas molecules randomly striking the detector entrance. Consequently, a detector capable of extracting the relatively weak reflected beam signal from the stronger background gas signal must be used. The AEDC molecular beam generation system is capable of producing beams several orders of magnitude more intense than the background gas, and a commercially available ionization gage can be used as a total beam intensity detector (see Section IV). However, a reflected beam flux of  $10^{-3}$  times the total incident beam flux will pass through the detector entrance for diffuse reflection at the surface when a detector with an entrance diameter of 4 mm is mounted 100 mm from the surface. The reflected beam intensity will also be a function of the surface capture coefficient; and by applying Eq. (6), the fractional

decrease in reflected beam flux can be determined. For a capture coefficient of 0.99, this fraction is  $10^{-2}$ . Under these conditions the detector is required to measure intensities  $10^{-5}$  times the total beam intensity entering the test chamber. As shown in Section 6.1, the AEDC beam generating system has a practical operating range from  $10^{14}$  to  $10^{16}$  molecules/sec/cm<sup>2</sup>. This requires measurement of reflected beam intensities from  $10^9$  to  $10^{11}$  molecules/sec/cm<sup>2</sup>. At a test chamber pressure of  $10^{-8}$  torr, the background gas impingement rate is about  $10^{12}$  molecules per sec/cm<sup>2</sup>. The detector is then required to produce signals proportional to beam intensities from one to three orders of magnitude below background gas intensities.

#### 6.2.1.2 Modulated Beam Detector

Several research groups have for many years used what is generally referred to as modulated beam techniques to detect the weak signals produced by gas molecules scattered from solid surfaces (Ref. 14). The beam to be detected is mechanically pulsed by passing it through a rotating slotted disc turning at a fixed frequency. This technique provides a means of recovering a signal hidden in background noise by using a-c amplification of the desired signal at one frequency and rejecting the noise at other frequencies. A mass spectrometer can be used as the signal source to provide a further gain in sensitivity by rejecting all signals from mass numbers other than that of the test gas. A detector incorporating these features has been developed at AEDC, and its performance has been experimentally determined. This detector has satisfied the requirements listed in Section 6.2.1.1 by recovering beam signals from two to three orders of magnitude below the total background gas intensity level.

### 6.3 OTHER BEAM APPLICATIONS

The aerodynamic beam system with its associated detector makes a versatile apparatus for application to a variety of gas-surface and gas-gas interaction studies. The mechanism of adsorption pumping as well as cryopumping can be readily investigated over a wide range of gas and surface temperatures. Other gas surface phenomena, such as evaporation and sputtering, can be studied using beam techniques. Gas-gas interactions involved in chemical processes and the measurement of scattering cross sections are studies for which intersecting molecular beams are particularly well suited.

A method is currently under development to measure the energy level of molecules scattered from solid surfaces. This energy

information will make possible studies of thermal accommodation coefficients, satellite drag coefficients, and rarefied gas flow phenomena in general.

## SECTION VII CONCLUDING REMARKS

An aerodynamic molecular beam chamber has been assembled and operated at AEDC. Cryopumping was successfully used to produce intense molecular beams by providing large pumping speeds and by reducing the scattering caused by the background gas. A maximum beam intensity of  $2.0 \times 10^{20}$  CO<sub>2</sub> molecules per second per steradian has been measured at a source pressure of 3400 torr. Cryogenic cooling of the beam skimmer resulted in large increases in the beam intensities, but the duration of the increase was very short.

A modulated beam detection system has been developed to provide the capability of detecting weak beam signals hidden in background noise.

The aerodynamic beam and modulated beam detector are to be used to investigate the cryopumping phenomena on the microscopic scale and to provide capture coefficient data for immediate application to the requirements of space simulation.

Molecular beam techniques have also been developed at AEDC and other laboratories for investigation of a wide spectrum of particle-surface interaction processes, such as adsorption, momentum exchange, energy exchange, and evaporation.

## REFERENCES

1. Kantrowitz, A. and Grey, J. "A High Intensity Source for the Molecular Beam." Review of Scientific Instruments, Vol. 22, May 1951, p. 328.
2. Ramsey, N. F. Molecular Beams. Clarendon Press, London, 1956.
3. Parker, H. M., Kuhlthau, A. R., Zapata, R. N., and Scott, J. E., Jr. "The Application of Supersonic Beam Sources to Low Density, High Velocity Experimentation." Rarefied Gas Dynamics, edited by F. M. Devienne, Pergamon Press, New York, 1960.

4. Knuth, E. L. "Status Report on the Development of a High-Speed High-Intensity Molecular Beam." University of California, Department of Engineering Report No. 63-30, 1963.
5. Fenn, John B. and Deckers, Jacques. "Molecular Beams from Nozzle Sources." Rarefied Gas Dynamics, Third Symposium, edited by J. A. Laurmann, Academic Press, New York, 1963.
6. Bier, K. and Hagena, O. "Influence of Shock Waves on Generation of High-Intensity Molecular Beams by Nozzles." Rarefied Gas Dynamics, Third Symposium, edited by J. A. Laurmann, Academic Press, New York, 1963.
7. Greene, Frank T. and Milne, Thomas A. "Mass Spectrometric Detection of Polymers in Supersonic Molecular Beams." Journal of Chemical Physics, Vol. 40, 1964, p. 3150.
8. Scott, John E., Jr. and Drewry, J. E. "Characteristics of Aerodynamic Molecular Beams." Rarefied Gas Dynamics, Third Symposium, edited by J. A. Laurmann, Academic Press, New York, 1963.
9. Sherman, F. S. "Self-Similar Development of Inviscid Hypersonic Free-Jet Flows." Fluid Mechanics Technical Report 6-90-93-61, Lockheed Missiles and Space Company, 1963.
10. Hodgman, C. D. Handbook of Chemistry and Physics. Chemical Rubber Publishing Company, Cleveland, 1957.
11. Knuth, E. L. "Rotational and Translational Relaxation Effects in Low-Density Hypersonic Free Jets." University of California, Department of Engineering Report No. 64-53, 1964.
12. Anderson, J. B. and Fenn, J. B. "Background and Sampling Effects in Free Jet Studies by Molecular Beam Measurements." International Symposium on Rarefied Gas Dynamics, Fourth, edited by J. A. Laurmann, Academic Press, New York, 1964.
13. Mayer, E., Tracy, R., Collins, J. A., and Triplett, J. J. "Condensation of Rarefied Supersonic Flow Incident on a Cold Flat Plate." International Symposium on Rarefied Gas Dynamics, Fourth, edited by J. A. Laurmann, Academic Press, New York, 1964.
14. Holister, G. S., Brackmann, R. F., and Fite, W. L. "The Use of Modulated Atomic-Beam Techniques for the Study of Space-Flight Problems." Planetary and Space Science, Vol. 3, 1961, p. 162.



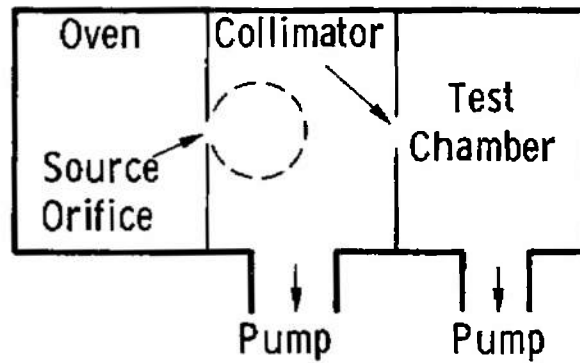


Fig. 1 Oven Beam Generator

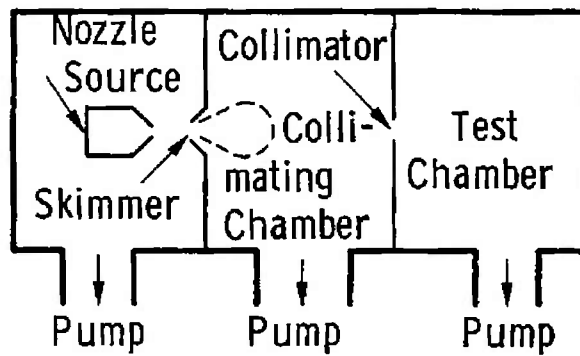


Fig. 2 Aerodynamic Beam Generator

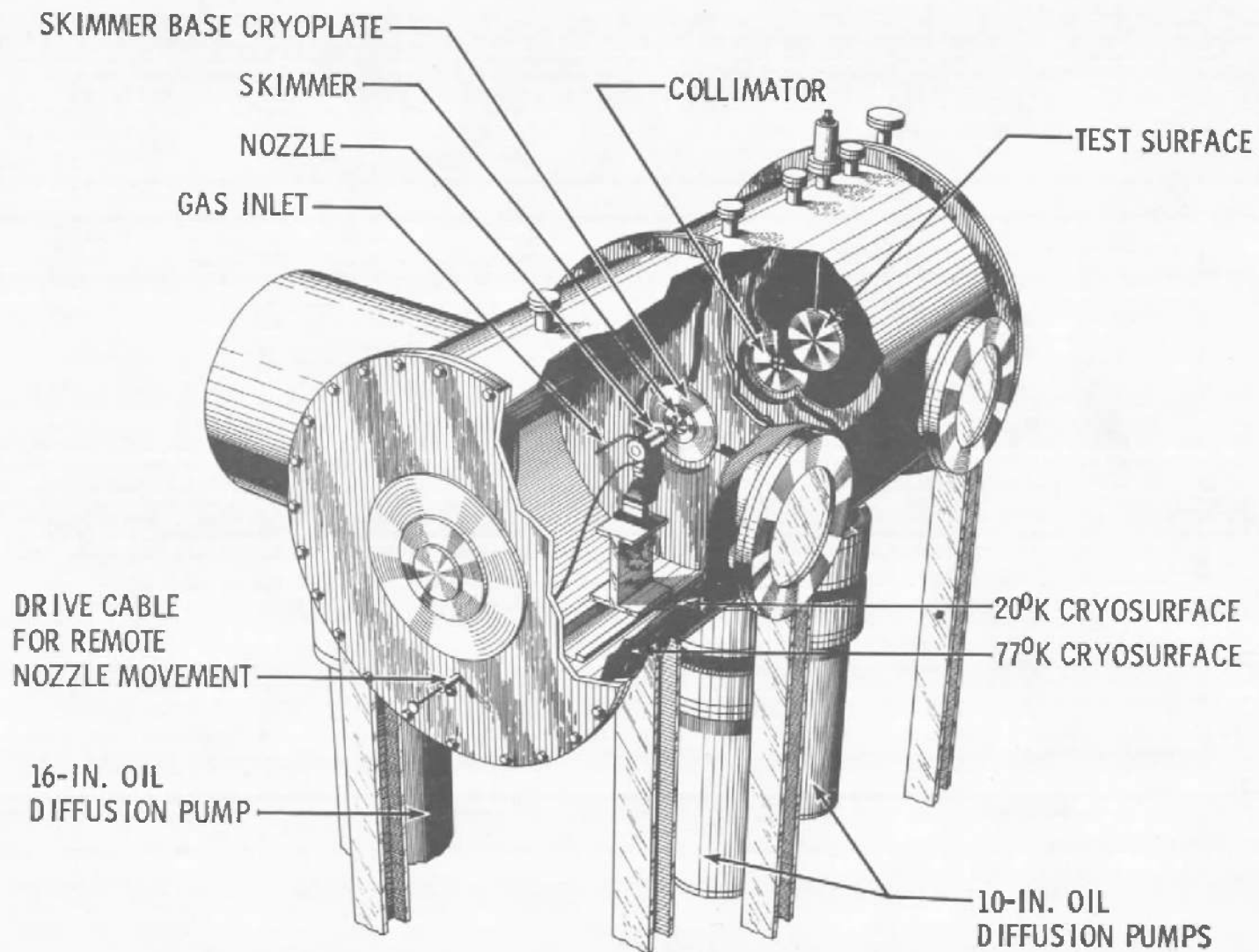


Fig. 3 Molecular Beam Chamber

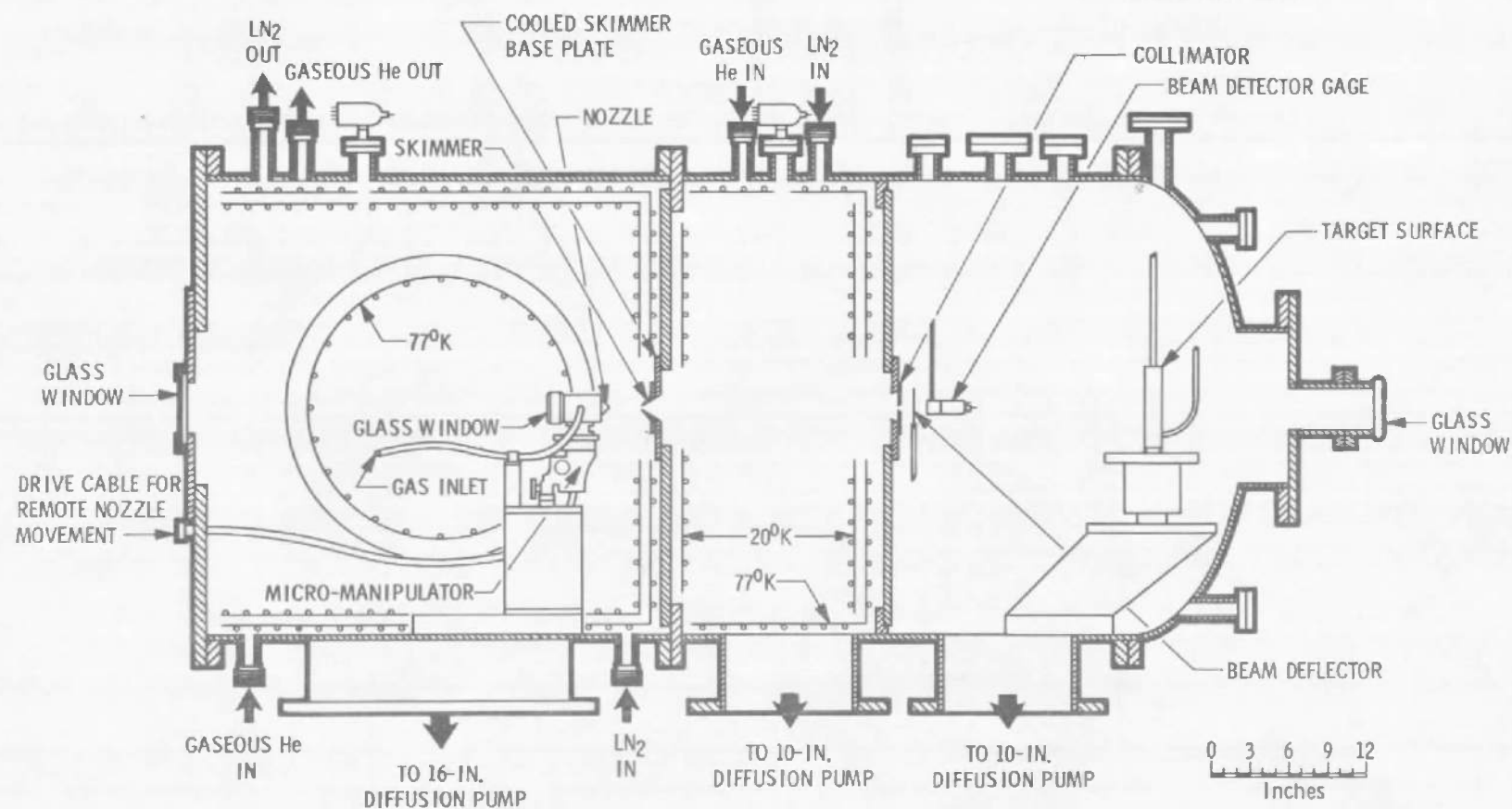


Fig. 4 Schematic of Aerodynamic Molecular Beam Chamber

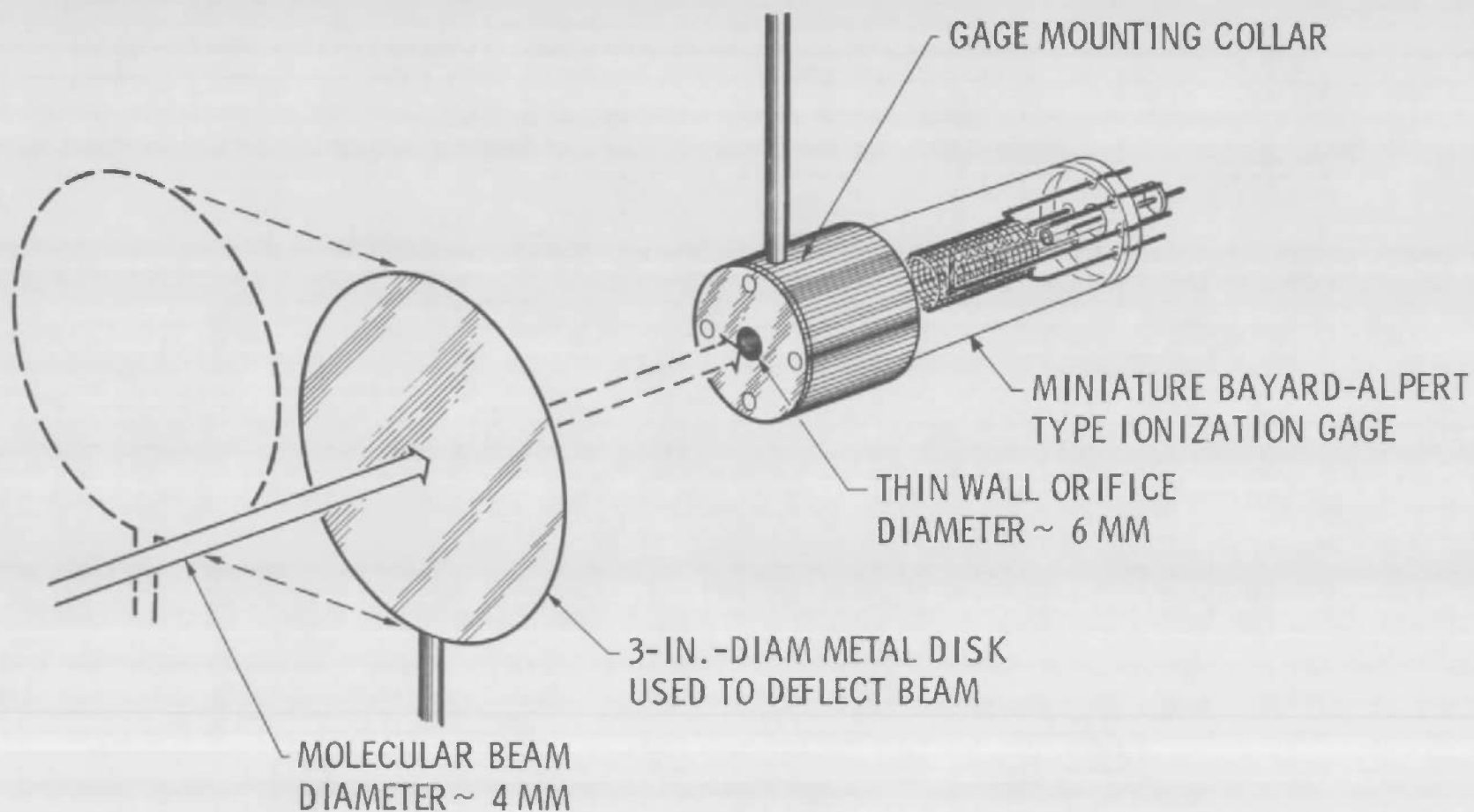


Fig. 5 Molecular Beam Detector

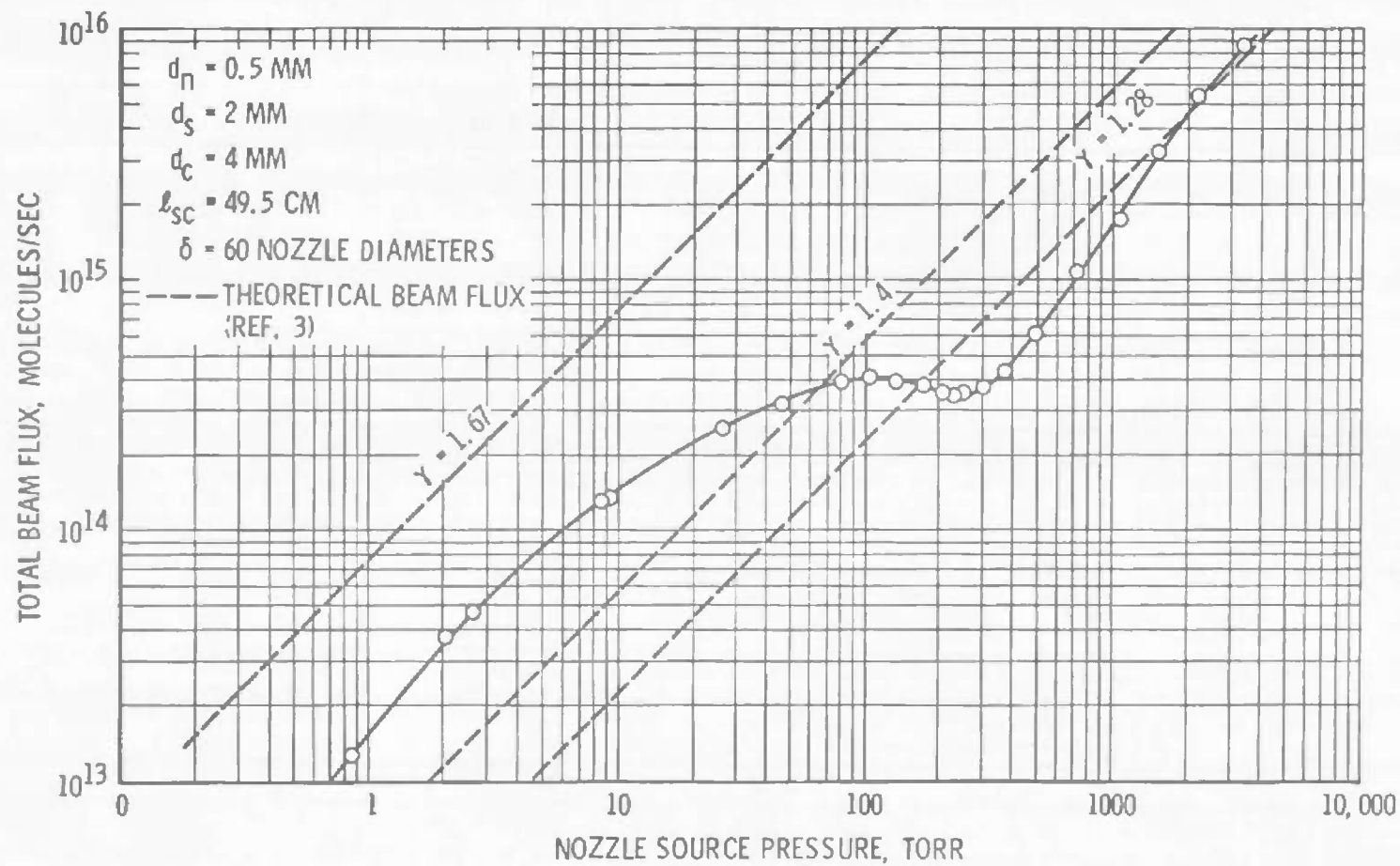
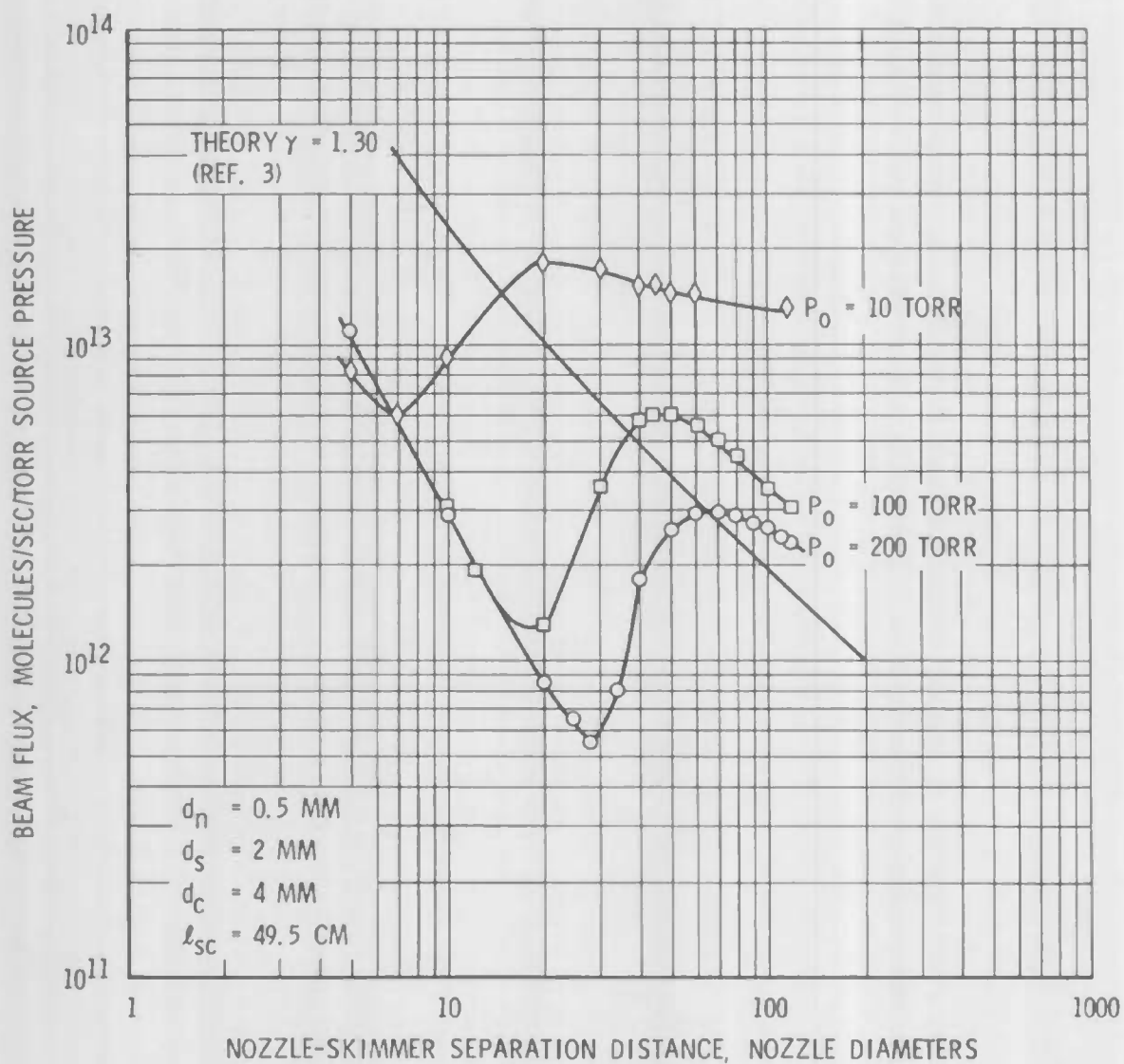


Fig. 6 Typical CO<sub>2</sub> Beam Performance Data

Fig. 7 Effect of Nozzle-Skimmer Separation Distance,  $\text{CO}_2$

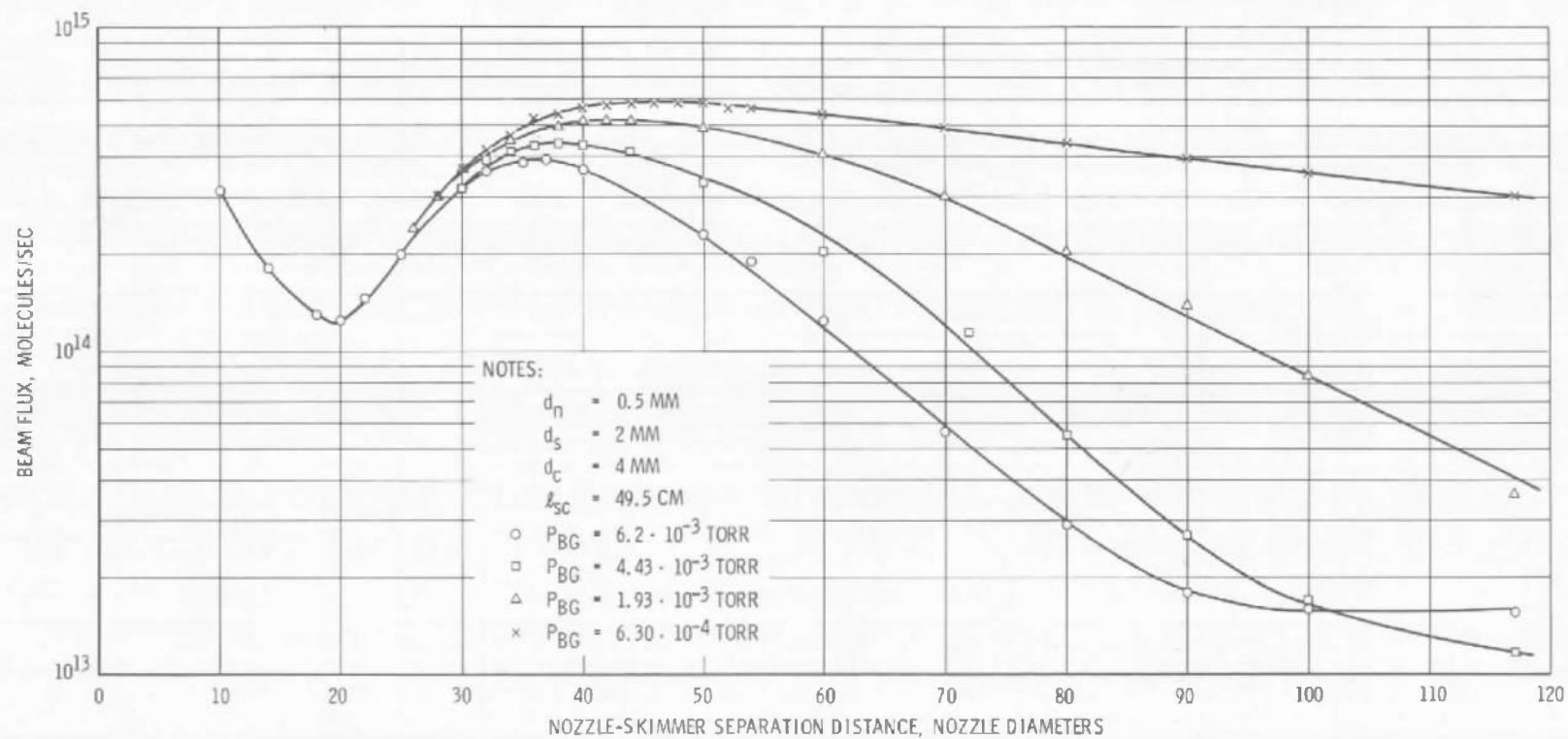
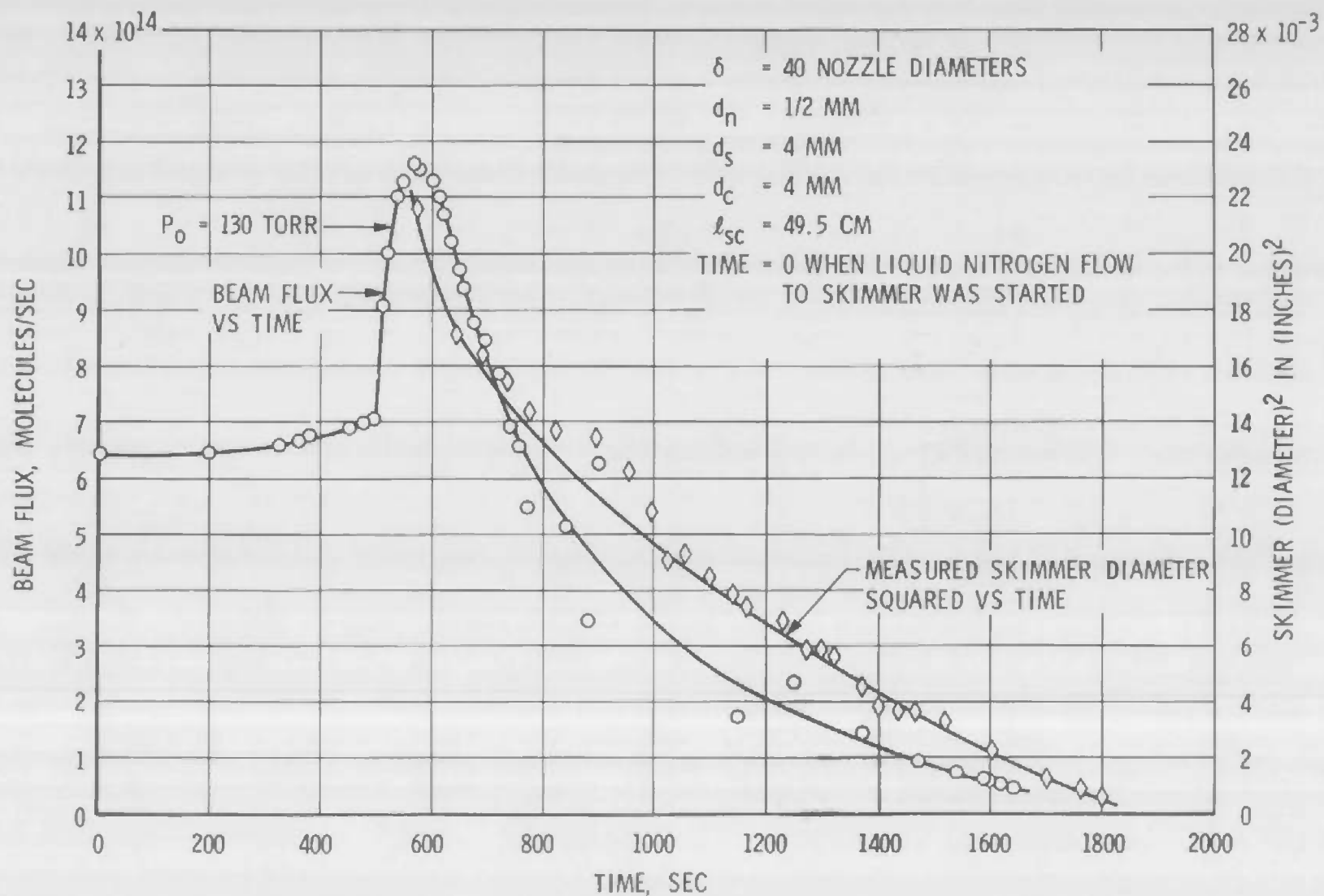


Fig. 8 Background Gas Scattering for 100-torr CO<sub>2</sub> Source Pressure

Fig. 9 Cold Skimmer Effects, CO<sub>2</sub>



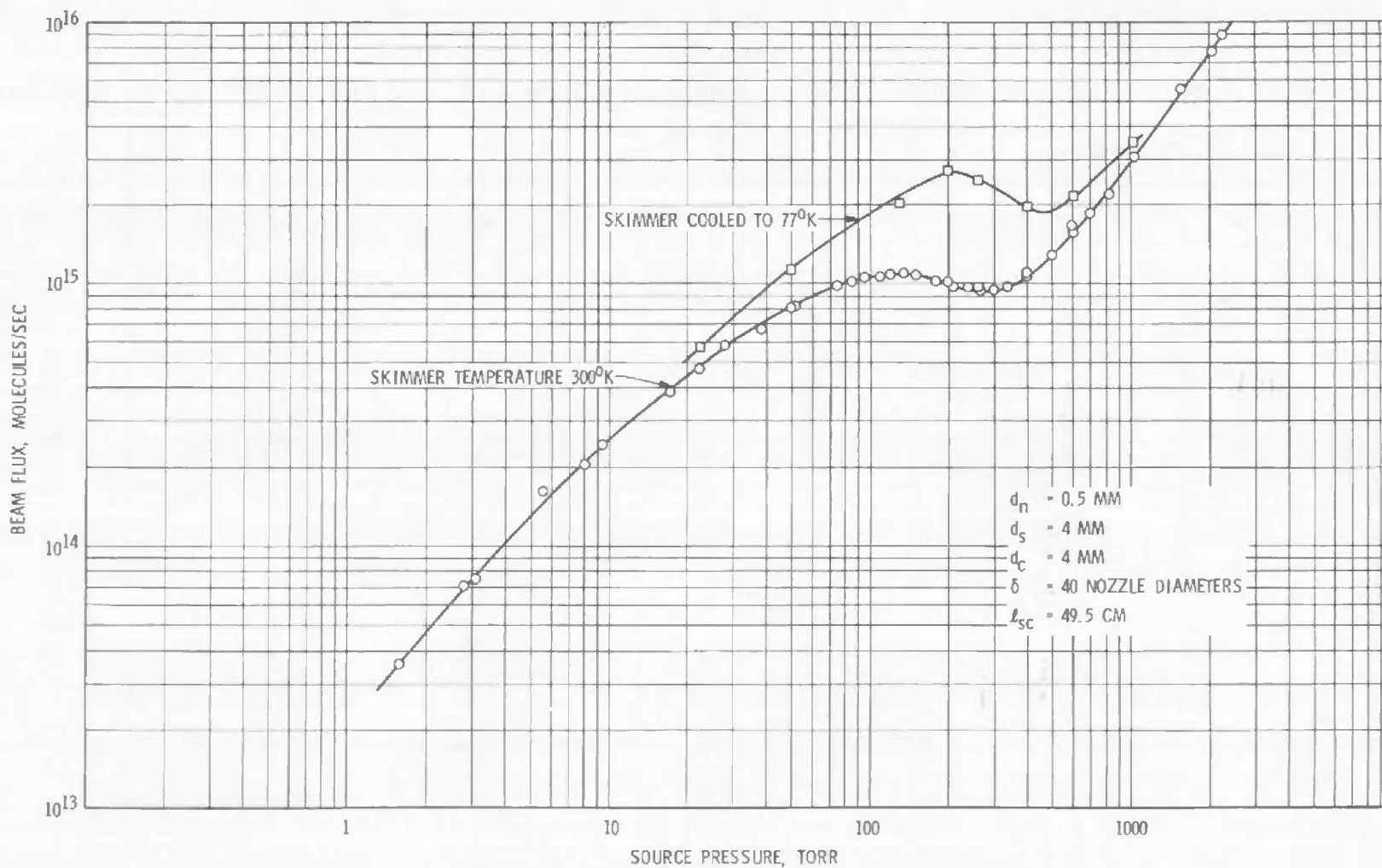


Fig. 10 Beam Performance with Variable Skimmer Temperature, CO<sub>2</sub>

TABLE I  
TYPICAL TEST DATA

$P_0$ , torr	$\delta$ , nozzle diameters	$P_n$ , torr	$P_c$ , torr	$P_t$ , torr	$\Delta P_d$ , torr	$K_d$ , mol/sec/torr	$\dot{N}$ , mol/sec
0.89	60 ↓	$9.0 \times 10^{-7}$	$3.3 \times 10^{-7}$	$1.2 \times 10^{-9}$	$7.9 \times 10^{-8}$	$1.565 \times 10^{20}$ ↓	$1.20 \times 10^{13}$
2.09		$9.0 \times 10^{-7}$	$3.7 \times 10^{-7}$	↓	$2.4 \times 10^{-7}$		$3.76 \times 10^{13}$
2.68		$8.8 \times 10^{-7}$	$2.8 \times 10^{-7}$	↓	$3.0 \times 10^{-7}$		$4.70 \times 10^{13}$
8.75		$2.2 \times 10^{-6}$	$4.0 \times 10^{-7}$	↓	$8.3 \times 10^{-7}$		$1.30 \times 10^{14}$
9.50		$2.4 \times 10^{-6}$	$4.3 \times 10^{-7}$	↓	$8.9 \times 10^{-7}$		$1.39 \times 10^{14}$
27.0		$6.6 \times 10^{-6}$	$6.2 \times 10^{-7}$	$1.5 \times 10^{-9}$	$1.65 \times 10^{-6}$		$2.58 \times 10^{14}$
47.5		$6.2 \times 10^{-6}$	$7.3 \times 10^{-7}$	↓	$2.05 \times 10^{-6}$		$3.21 \times 10^{14}$
81.5		$6.6 \times 10^{-6}$	$6.4 \times 10^{-7}$	↓	$2.50 \times 10^{-6}$		$3.92 \times 10^{14}$
111		$8.1 \times 10^{-6}$	$9.1 \times 10^{-7}$	↓	$3.64 \times 10^{-6}$		$5.70 \times 10^{14}$
180		$1.2 \times 10^{-5}$	$8.8 \times 10^{-7}$	↓	$2.40 \times 10^{-6}$		$3.76 \times 10^{14}$
184		$1.2 \times 10^{-5}$	$8.0 \times 10^{-7}$	$1.6 \times 10^{-9}$	$2.44 \times 10^{-6}$		$3.82 \times 10^{14}$
108		$8.8 \times 10^{-6}$	$4.8 \times 10^{-7}$	↓	$2.62 \times 10^{-6}$		$4.10 \times 10^{14}$
136		$1.1 \times 10^{-5}$	$5.2 \times 10^{-7}$	↓	$2.50 \times 10^{-6}$		$3.91 \times 10^{14}$
255		$1.6 \times 10^{-5}$	$7.3 \times 10^{-7}$	↓	$2.30 \times 10^{-6}$		$3.60 \times 10^{14}$
377		$1.9 \times 10^{-5}$	$8.8 \times 10^{-7}$	↓	$2.80 \times 10^{-6}$		$4.37 \times 10^{14}$
302		$2.3 \times 10^{-5}$	$5.8 \times 10^{-7}$	$2.1 \times 10^{-9}$	$2.40 \times 10^{-6}$		$3.76 \times 10^{14}$
215		$1.1 \times 10^{-5}$	$4.3 \times 10^{-7}$	↓	$2.24 \times 10^{-6}$		$3.51 \times 10^{14}$
237		$1.1 \times 10^{-5}$	$4.5 \times 10^{-7}$	↓	$2.23 \times 10^{-6}$		$3.49 \times 10^{14}$
496		$1.4 \times 10^{-5}$	$6.8 \times 10^{-7}$	↓	$3.90 \times 10^{-6}$		$6.11 \times 10^{14}$
739		$1.8 \times 10^{-5}$	$6.8 \times 10^{-7}$	$3.3 \times 10^{-9}$	$6.70 \times 10^{-6}$		$1.05 \times 10^{15}$
1010		$1.6 \times 10^{-5}$	$6.5 \times 10^{-7}$	↓	$1.1 \times 10^{-5}$		$1.72 \times 10^{15}$
1530		$1.4 \times 10^{-5}$	$6.8 \times 10^{-7}$	↓	$2.1 \times 10^{-5}$		$3.29 \times 10^{15}$
2260		$1.5 \times 10^{-5}$	$6.5 \times 10^{-7}$	$5.4 \times 10^{-9}$	$3.5 \times 10^{-5}$		$5.47 \times 10^{15}$
3400		$9.0 \times 10^{-6}$	$5.1 \times 10^{-7}$	$5.6 \times 10^{-9}$	$5.65 \times 10^{-5}$		$8.85 \times 10^{15}$

NOTES:  $d_n = 1/2$  mm $T_0 = 300^\circ\text{K}$  $d_s = 2$  mm $l_{sc} = 49.5$  cm $d_c = 4$  mmTest gas is  $\text{CO}_2$ .

UNCLASSIFIED

Security Classification

## DOCUMENT CONTROL DATA - R&amp;D

(Security classification of title, body of abstract and indexing annotation must be entered when the overall report is classified)

1 ORIGINATING ACTIVITY (Corporate author) Arnold Engineering Development Center ARO, Inc., Operating Contractor Arnold Air Force Station, Tennessee		2a REPORT SECURITY CLASSIFICATION UNCLASSIFIED	
		2b GROUP N/A	
3 REPORT TITLE DESCRIPTION AND PERFORMANCE OF A MOLECULAR BEAM CHAMBER USED FOR CRYOPUMPING AND ADSORPTION PUMPING STUDIES			
4 DESCRIPTIVE NOTES (Type of report and inclusive dates) N/A			
5 AUTHOR(S) (Last name, first name, initial) R. F. Brown and J. H. Heald, Jr., ARO, Inc.			
6 REPORT DATE October 1966		7a TOTAL NO OF PAGES 33	7b NO OF REFS 14
8a CONTRACT OR GRANT NO. AF40(600)-1200		9a ORIGINATOR'S REPORT NUMBER(S) AEDC-TR-66-135	
b PROJECT NO 8951			
c Program Element 61445014		9b OTHER REPORT NO(S) (Any other numbers that may be assigned this report) N/A	
d			
10 AVAILABILITY/LIMITATION NOTICES Distribution of this document is unlimited.			
11 SUPPLEMENTARY NOTES Available in DDC		12 SPONSORING MILITARY ACTIVITY Arnold Engineering Development Center, Air Force Systems Command, Arnold AF Station, Tennessee	
13 ABSTRACT An aerodynamic molecular beam chamber has been constructed and operated at Arnold Engineering Development Center. Design criteria, performance data, and space simulation applications are discussed in this report. Cryopumping was utilized to provide the required pumping speed and to reduce the scattering of the beam by the background gas. A maximum beam intensity of $2.0 \times 10^{20}$ CO <sub>2</sub> molecules per second per steradian was measured. The beam is now being used to study basic cryopumping phenomena on a microscopic scale and to provide capture coefficient data for immediate application in the design of cryopumping systems for space simulation chambers.			

14	KEY WORDS	LINK A		LINK B		LINK C	
		ROLE	WT	ROLE	WT	ROLE	WT
	/ molecular beam chamber design criteria performance space simulation 2 cryopumping pumping speed 4 capture coefficient data oven beam generators 3 aerodynamic <sup>molecular</sup> beam generators chambers 5 Adsorption pumping						

15-2

INSTRUCTIONS

1. **ORIGINATING ACTIVITY:** Enter the name and address of the contractor, subcontractor, grantee, Department of Defense activity or other organization (corporate author) issuing the report.

2a. **REPORT SECURITY CLASSIFICATION:** Enter the overall security classification of the report. Indicate whether "Restricted Data" is included. Marking is to be in accordance with appropriate security regulations.

2b. **GROUP:** Automatic downgrading is specified in DoD Directive 5200.10 and Armed Forces Industrial Manual. Enter the group number. Also, when applicable, show that optional markings have been used for Group 3 and Group 4 as authorized.

3. **REPORT TITLE:** Enter the complete report title in all capital letters. Titles in all cases should be unclassified. If a meaningful title cannot be selected without classification, show title classification in all capitals in parenthesis immediately following the title.

4. **DESCRIPTIVE NOTES:** If appropriate, enter the type of report, e.g., interim, progress, summary, annual, or final. Give the inclusive dates when a specific reporting period is covered.

5. **AUTHOR(S):** Enter the name(s) of author(s) as shown on or in the report. Enter last name, first name, middle initial. If military, show rank and branch of service. The name of the principal author is an absolute minimum requirement.

6. **REPORT DATE:** Enter the date of the report as day, month, year, or month, year. If more than one date appears on the report, use date of publication.

7a. **TOTAL NUMBER OF PAGES:** The total page count should follow normal pagination procedures, i.e., enter the number of pages containing information.

7b. **NUMBER OF REFERENCES:** Enter the total number of references cited in the report.

8a. **CONTRACT OR GRANT NUMBER:** If appropriate, enter the applicable number of the contract or grant under which the report was written.

8b, 8c, & 8d. **PROJECT NUMBER:** Enter the appropriate military department identification, such as project number, subproject number, system numbers, task number, etc.

9a. **ORIGINATOR'S REPORT NUMBER(S):** Enter the official report number by which the document will be identified and controlled by the originating activity. This number must be unique to this report.

9b. **OTHER REPORT NUMBER(S):** If the report has been assigned any other report numbers (either by the originator or by the sponsor), also enter this number(s).

10. **AVAILABILITY/LIMITATION NOTICES:** Enter any limitations on further dissemination of the report, other than those imposed by security classification, using standard statements such as:

(1) "Qualified requesters may obtain copies of this report from DDC."

(2) "Foreign announcement and dissemination of this report by DDC is not authorized."

(3) "U. S. Government agencies may obtain copies of this report directly from DDC. Other qualified DDC users shall request through \_\_\_\_\_."

(4) "U. S. military agencies may obtain copies of this report directly from DDC. Other qualified users shall request through \_\_\_\_\_."

(5) "All distribution of this report is controlled. Qualified DDC users shall request through \_\_\_\_\_."

If the report has been furnished to the Office of Technical Services, Department of Commerce, for sale to the public, indicate this fact and enter the price, if known.

11. **SUPPLEMENTARY NOTES:** Use for additional explanatory notes.

12. **SPONSORING MILITARY ACTIVITY:** Enter the name of the departmental project office or laboratory sponsoring (paying for) the research and development. Include address.

13. **ABSTRACT:** Enter an abstract giving a brief and factual summary of the document indicative of the report, even though it may also appear elsewhere in the body of the technical report. If additional space is required, a continuation sheet shall be attached.

It is highly desirable that the abstract of classified reports be unclassified. Each paragraph of the abstract shall end with an indication of the military security classification of the information in the paragraph, represented as (TS), (S), (C), or (U).

There is no limitation on the length of the abstract. However, the suggested length is from 150 to 225 words.

14. **KEY WORDS:** Key words are technically meaningful terms or short phrases that characterize a report and may be used as index entries for cataloging the report. Key words must be selected so that no security classification is required. Identifiers, such as equipment model designation, trade name, military project code name, geographic location, may be used as key words but will be followed by an indication of technical context. The assignment of links, rules, and weights is optional.